Supporting Information

Enhanced stability of Vanadium-doped Li$_{1.2}$Ni$_{0.16}$Co$_{0.08}$Mn$_{0.56}$O$_2$ cathode materials for superior Li-ion batteries

Miaomiao Zhou [a,†], Jianjun Zhao [b,†], Xiaodong Wang [a,†], Ji Shen [a], Jin-Lin Yang [c,d], Wenhao Tang [a], Yirui Deng [a], Shi-Xi Zhao[c,*], Ruiping Liu[a,*]

[a] School of ChemicaL & Environmental Engineering, China University of Mining and Technology (Beijing), Beijing 100083, PR China.

[b] State Key Laboratory of Chemical Resources Engineering, Beijing Advanced Innovation Center for Soft Matter Science and Engineering, College of Chemistry, Beijing University of Chemical Technology, Beijing 100029, China.

[c] Tsinghua Shenzhen International Graduate School, Tsinghua University, Shenzhen, 518055, China.

[d] School of Materials Science and Engineering, Tsinghua University, Beijing, 100084, China.

Table S1. Lattice parameters of pristine, V-0.5%,V-0.2%, V-1%,V-2% and V-5% samples.

Samples	a(Å)	c(Å)	c/a	V (Å³)	$I_{(003)}/I_{(104)}$
Pristine	2.8751	14.2475	4.9554	101.99	1.323
V-0.5%	2.8715	14.2674	4.9686	101.88	1.390
V-1%	2.8546	14.2691	4.9986	100.74	1.417
V-2%	2.8549	14.2659	4.9969	100.75	1.319
V-5%	2.8863	14.2052	4.9215	102.48	1.271
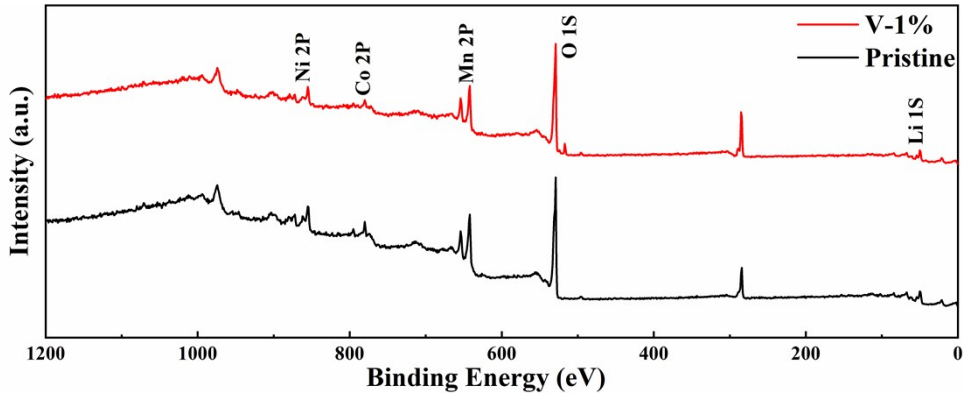
Fig. S1. XPS images for the pristine and V-1% samples.

Table S2. Percentage of Mn^{3+} ions in the pristine material and V-1%.

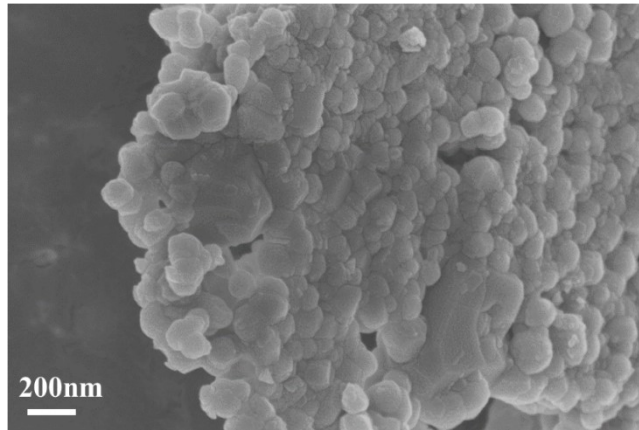| Pristine	Position	Area	V-1%	Position	Area
Mn^{4+}	642.68	86566.36	Mn^{4+}	642.67	48367.46
Mn^{3+}	641.49	20474.39	Mn^{3+}	641.51	22423.2
Mn^{3+} in Mn		19.12%	Mn^{3+} in Mn		31.67%

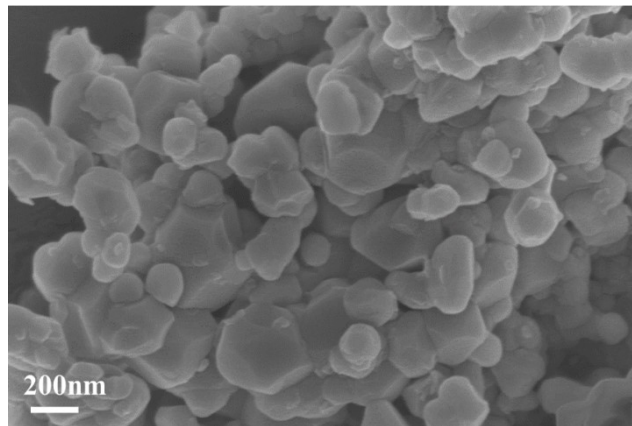**Fig. S2.** SEM images of V-5% sample.

Fig. S3. SEM images of V-0.05% sample.
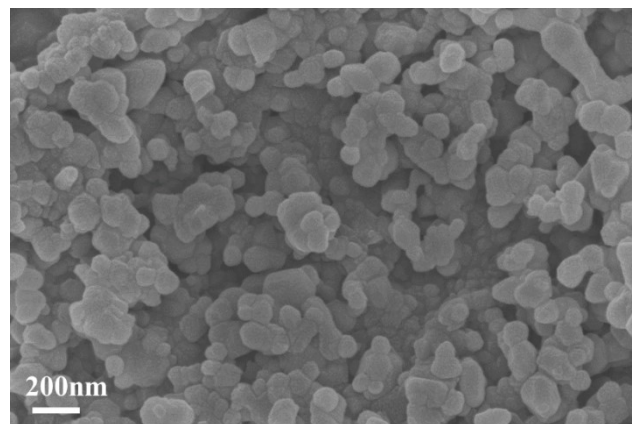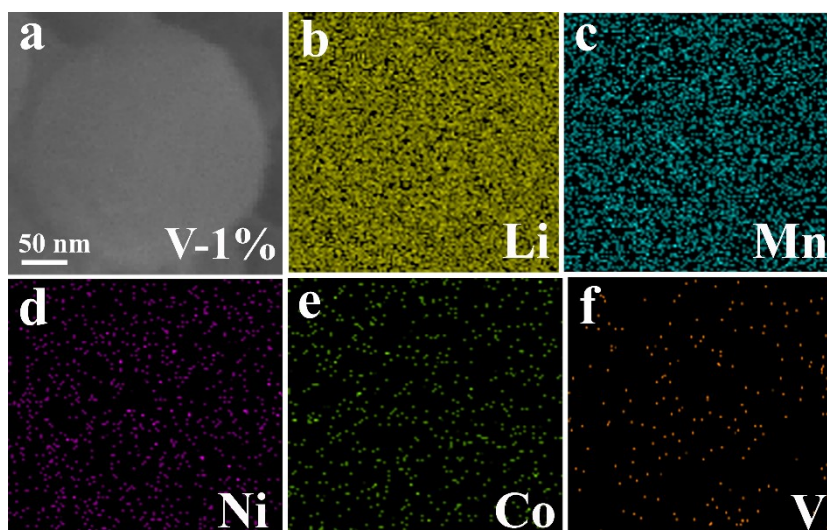

Fig. S4. SEM images of V-2% sample

Fig. S5. SEM images of V-1% (a); EDS-mapping of Li (b), Mn (c), Ni (d), Co (e), and V (f).
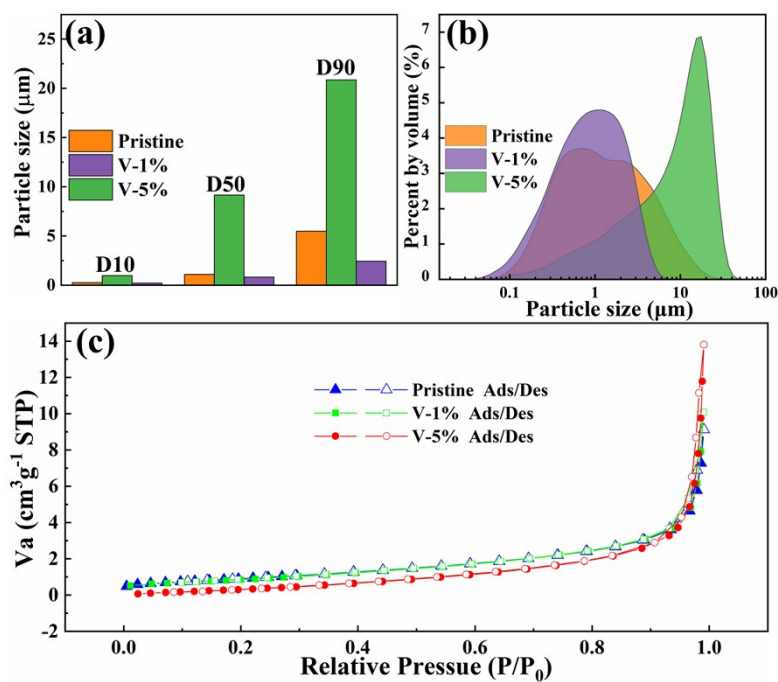

Fig. S6. (a, b) Secondary particle size distribution of the pristine, V-1%, and V-5% samples, D90, D50 and D10 are the equivalent diameters (average particle size) of the largest particles in the distribution curve at a cumulative distribution of 90%, 50% and 10%, respectively. (c) Nitrogen adsorption and desorption isotherms of the pristine, V-1%, and V-5% samples.
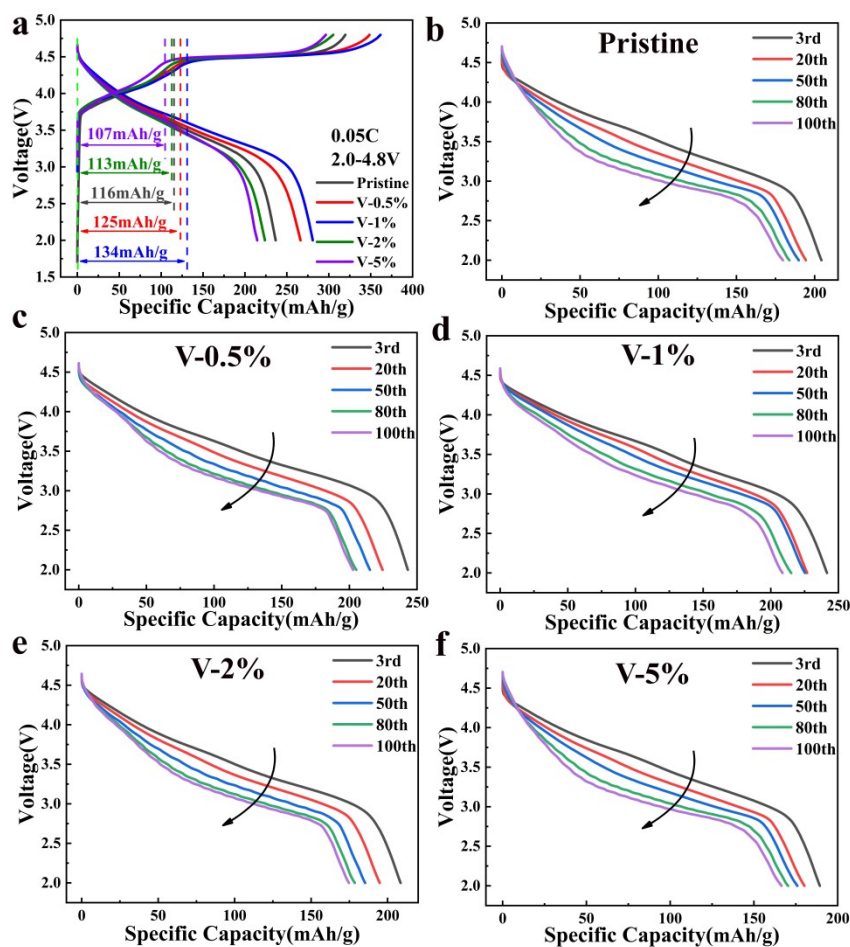
Fig. S7. Initial galvanostatic charge/discharge profiles of the pristine, V-0.5%, V-1%, V-2%, and V-5% samples at the current density of 0.05 C (1 C = 250 mAg^{-1}) between 2.0 and 4.8 V (a); the charge/discharge curves of pristine, V-0.5%, V-1%, ,V-2%, and V-5% samples (b-f).

Table S3. Initial charge/discharge data for the pristine, V-0.5%, V-1%, V-2% and V-5% electrodes at the current density of 0.05 C between 2.0 and 4.8 V.

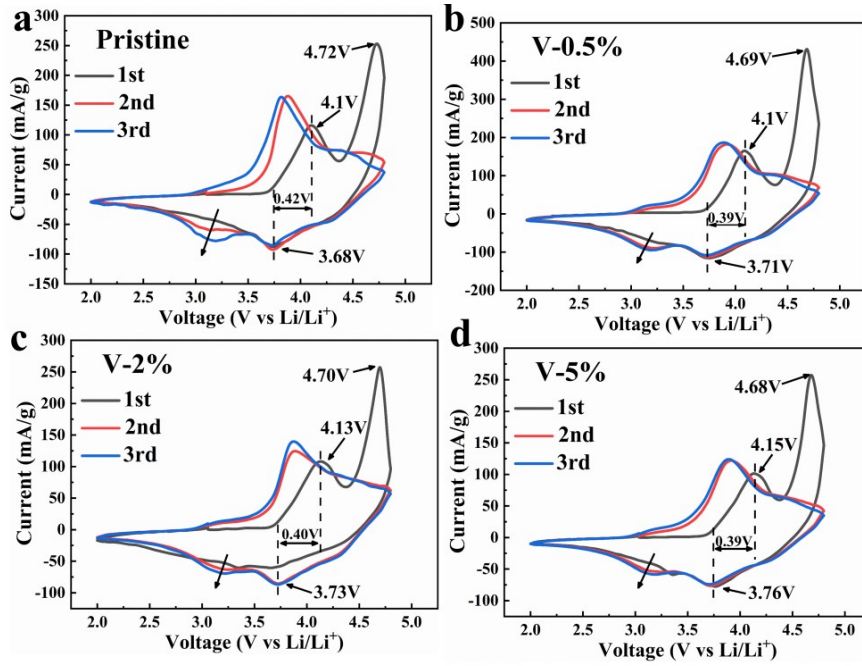| Sample	Charge capacity (mA·g^{-1})	Discharge capacity (mAh·g^{-1})	Sloping area (mAh·g^{-1})	Platform area (mAh·g^{-1})	Coulomb efficiency (%)
Pristine	319.72	236.63	116.54	203.18	74.01
V-0.05%	348.63	266.25	125.12	223.51	76.37
V-1%	361.65	280.91	134.26	227.39	77.67
V-2%	305.21	223.81	113.67	191.54	73.33
V-5%	296.55	214.69	107.99	188.56	72.40

Fig. S8. Cyclic voltammetry curves of the pristine, V-0.5%, , V-2%, and V-5% (a-d) samples at
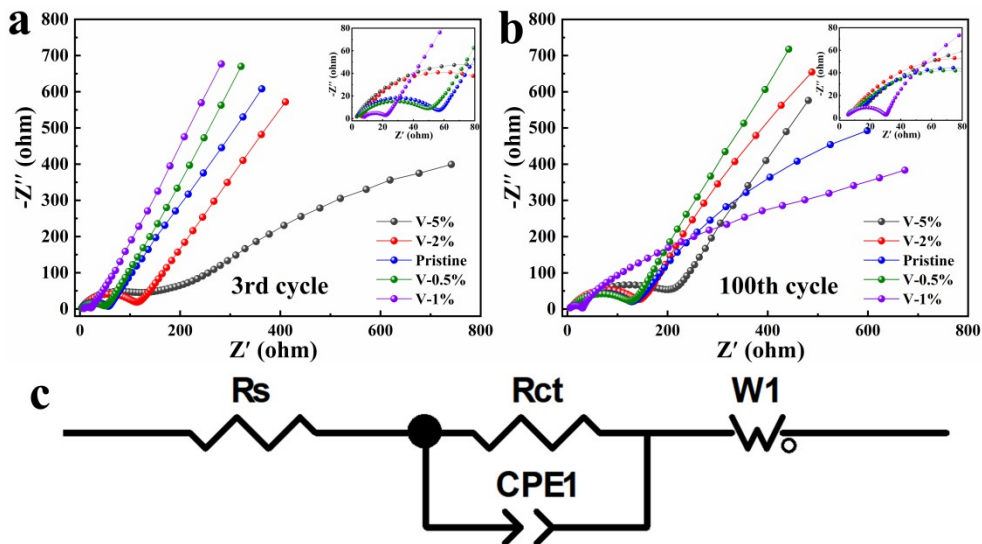
0.1 mV·s⁻¹.

Fig. S9. Nyquist plots of pristine, V-0.5%, V-1%, V-2%, and V-2% samples for the 3rd cycle (a);

Nyquist plots of pristine, V-0.5%, V-1%, V-2%, and V-2% samples for the 100th cycle (b).

Table S4 The Impedance data for the pristine,V-0.5%,V-1%,V-2% and V-2% electrodes for the 3rd and 100th cycles.

Samples	R_{ct} (Ω, 3rd cycle)	R_{ct} (Ω, 100th cycle)	R_s (Ω, 3rd cycle)	R_s (Ω, 3rd cycle)
Pristine	49.85	106.90	2.85	10.54
V-0.5%	45.15	116.00	3.33	5.77
V-1%	14.61	20.72	6.98	4.50
V-2%	105.9	126.8	6.28	4.50
V-5%	113.5	205.4	1.07	10.20

Table S5 Lattice parameters of pristine, V-1% and V-5% samples after cycles.

Samples	I(003)/I(104)
Pristine	1.392
V-1%	1.401
V-5%	0.880